ELSEVIER

Journal of Molecular Catalysis A: Chemical 138 (1999) 1–13

JOURNAL OF MOLECULAR CATALYSIS A: CHEMICAL

The photocatalytic autoxidation of sulfur oxoanions by water-soluble porphyrin complexes

Shen-Ming Chen *

Department of Chemical Engineering, National Taipei University of Technology, No. 1, Section 3, Chung-Hsiao East Road, Taipei 10643, Taiwan

Received 3 January 1997; accepted 26 March 1998

Abstract

The photocatalytic autoxidation of $S_4O_6^{2-}$ and $S_2O_3^{2-}$ by water-soluble porphyrin complexes Fe(2-TMPyP), Mn(4-TMPyP), and Co(2-TMPyP) were compared under illumination with a 419 nm visible light in oxygen-saturated aqueous solutions at room temperature. The process involves $S_2O_3^{2-}$ as an intermediate product and SO_4^{2-} is the final oxidation product. The trend in photocatalytic activity of the porphyrin complexes for $S_4O_6^{2-}$ oxidation is Co(2-TMPyP) > Mn(4-TMPyP) > Fe(2-TMPyP). For $S_2O_3^{2-}$ oxidation, the trend is Co(2-TMPyP) > Fe(2-TMPyP) > Mn(4-TMPyP).

Keywords: Photocatalytic autoxidation; Sulfur oxoanions; Porphyrin complexes

1. Introduction

$S_2O_3^{2-}$, $S_4O_6^{2-}$, and SO_3^{2-} are the intermediates of sulfide oxidation by oxygen. These compounds are found in partially oxidized sulfur in the processing of sulfide ores, and in the treatment of wastewater [1,2].

Porphyrin complexes resemble phthalocyanines [2] as active parts in visible light-driven processes. These complexes exhibit many photochemical applications [3–5]. The photocatalytic reaction by phthalocyanine complexes [6–10] and porphyrin complexes [11,12] were previously reported.

The photooxidation of SO_3^{2-} [13,14] and the photocatalytic autoxidation of SO_3^{2-} [15–17] and S^{2-} [2,9,18] have also been studied. The photodecomposition or photocatalytic oxidation of sulfite and sulfur oxoanions has potential utility in solving the environmental pollution problem [19].

This paper discuss the photocatalytic autoxidation of $S_4O_6^{2-}$ and $S_2O_3^{2-}$ under illumination with 419 nm light by water-soluble porphyrin complexes Fe(2-TMPyP), Mn(4-TMPyP), and

* Corresponding author.

1381-1169/99/$ - see front matter
PII: S1381-1169(98)00148-4

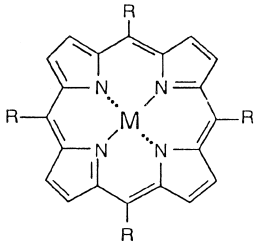

R	M	Abbreviation
	Fe	Fe(2-TMPyP)
	Co	Co(2-TMPyP)
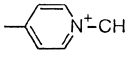	Mn	Mn(4-TMPyP)

Fig. 1. Structure of Fe(2-TMPyP), Co(2-TMPyP), Mn(4-TMPyP).

Co(2-TMPyP) (Fig. 1) in oxygen-saturated aqueous solution at room temperature.

2. Experimental

A sample of Fe^{III}(2-TMPyP) was prepared according to a literature method [20,21]. Pyrrole and 2-pyridine carboxaldehyde were refluxed in propionic acid to obtain the meso-tetrakis(2-pyridyl)porphyin (H_2(2-TPyP), $C_{40}N_8H_{26}$). Methylation was achieved by reacting H_2(2-TPyP) with neat dimethyl sulphate to form meso-tetrakis(*N*-methyl-2-pyridyl)porphyin ([H_2(2-TMPyP)]$(SO_4CH_3)^-$). Metallation was achieved by refluxing H_2(2-TMPyP) with $FeCl_2 \cdot H_2O$ in distilled water for 10 h. [Fe^{III}(2-TMPyP)]$^{5+}$ was precipitated by drops of saturated $NaClO_4$ solution and recrystalized with water. Co(2-TMPyP) was prepared through metallation by refluxing H_2(2-TMPyP) with $CoCl_2 \cdot 6H_2O$ by a literature method [22]. The products were identified by their UV–visible, IR, and NMR spectra. Mn(4-TMPyP) was purchased from Porphyrin Products (Logan, UT).

All chemicals were of analytical grade. Aqueous solutions were prepared with doubly distilled deionized water. Solutions were deoxygenated by purging with pre-purified nitrogen gas. Buffer solutions were prepared from H_2SO_4, KHP (potassium hydrogen phthalate), acetate, phosphate, borate, carbonate, and KOH for the pH range 0–14. The pH values were measured with a HANNA Model 8418 pH meter.

Irradiation was carried out on 15 ml quartz sample tube containing $S_4O_6^{2-}$ or $S_2O_3^{2-}$, and catalyst in buffer solution. The irradiation light was 419 nm 8 lamps (RPR-4190 A, 112 W) equipped with a Rayonet photochemical chamber reactor model RPR-100.

The thiosulfate and tetrathionate content were quantified by measuring the absorbance at $\lambda =$ 215 nm through the use of a flow system with a micro cell and a UV–visible detector. The sulfur oxoanions were also quantified by ion chromatography.

Electrochemistry was performed with a Bioanalytical system (West Lafayette, IN) Model CV-27 potentiostat and a BAS X-Y recorder. Cyclic voltammetry was conducted with the use of a three-electrode cell in which a BAS glassy carbon electrode (area 0.07 cm^2) was used as the working electrode. The glassy carbon electrode was polished with 0.05 μm alumina on Buehler felt pads and ultrasonicated for 1 min. The auxiliary compartment contained a platinum wire which was separated by a medium-sized glass frit. All cell potentials were taken with the use of a Ag/AgCl/KCl (saturated KCl solution) reference electrode. UV–visible spectra were measured with a Hitachi Model U-3200 Spectrophotometer.

The ion chromatograph used in the experiments was a Dionex Instruments ion chromatography DX-100 consisting of a pump, conductivity detector, an electrochemical detector, and a syringe loading system with 25-μl sample loop. The IC chromatograms were recorded using a

Spectra-Physics DataJet computing integrator. The columns used throughout were an IonPac AG4A guard column, an IonPac AS4A analytical column, and a self-regenerating suppressor column. Typical LC operational parameters were as follows: mobile phase was a Na_2CO_3 and $NaHCO_3$ buffer solution, mobile phase flow rate was 2 ml/min; the column temperature was at room temperature. These parameters were used for analyzing sulfate, sulfite and thiosulfate. Thiosulfate and $S_2O_6^{2-}$ were analyzed by an MPIC-NG1 guard column, an MPIC-NS1 analytical column, and a suppressor column.

3. Results and discussion

3.1. The photocatalytic autoxidation of $S_4O_6^{2-}$ by Co(2-TMPyP)

The decomposition of tetrathionate was carried out under oxygen at pH 9.0 in the presence and absence of Co(2-TMPyP) under illumina-

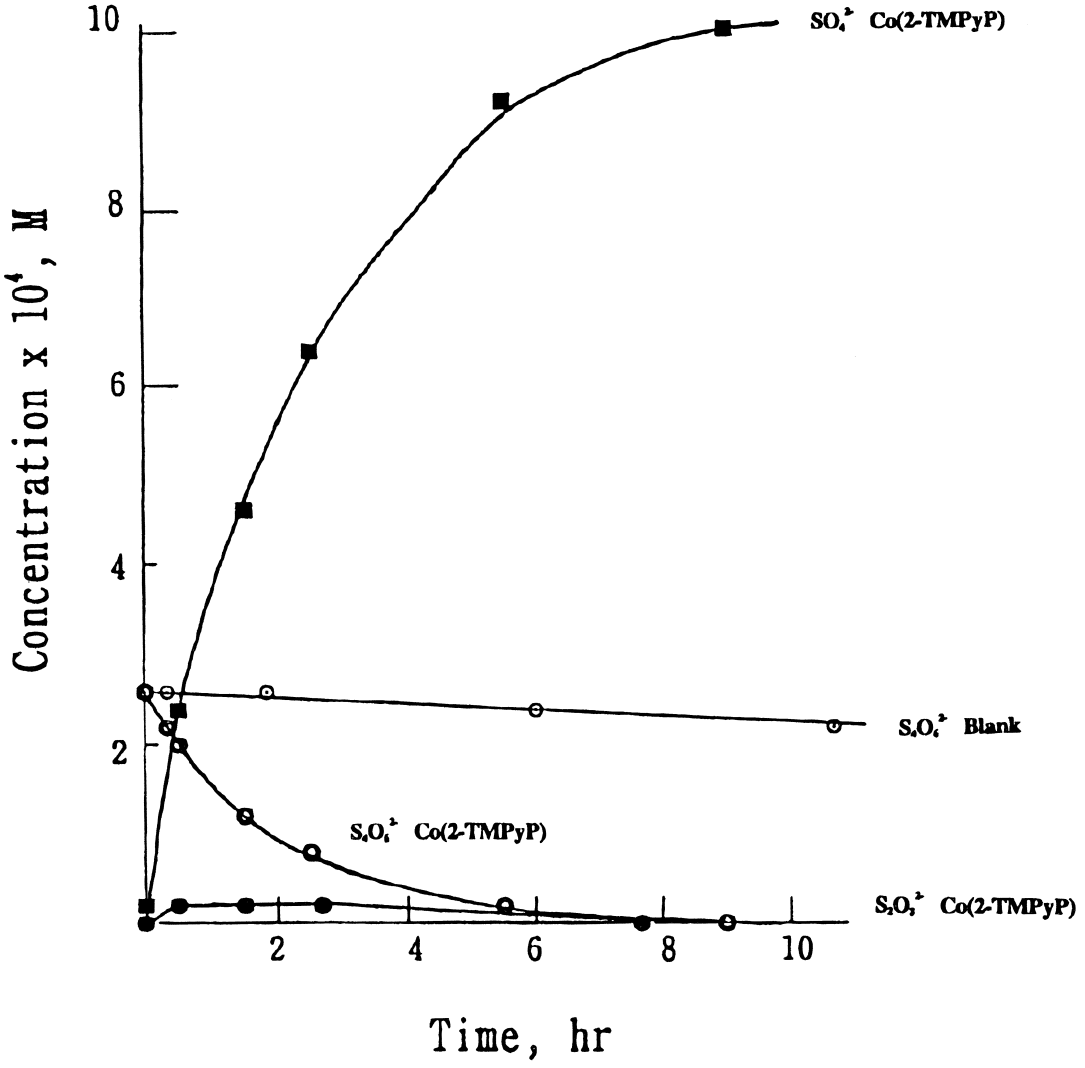

Fig. 2. Concentration of sulfur oxoanions vs. time of oxygen present at pH 9.0 borate buffer solution using 10^{-5} M of Co(2-TMPyP) with initial $[S_4O_6^{2-}] = 2.5 \times 10^{-4}$ M under illumination with 419 nm light. (⊙) $[S_4O_6^{2-}]$, (●) $[S_2O_3^{2-}]$, (■) $[SO_4^{2-}]$, (⊙) $[S_4O_6^{2-}]$ without Co(2-TMPyP).

tion with a 419 nm monochromatic light. Fig. 2 shows the disappearance of $S_4O_6^{2-}$ (⊙), the rise of SO_4^{2-} (■), and the presence of intermediate $S_2O_3^{2-}$ (●) during the catalytic process. The half-life of the decomposition of $S_4O_6^{2-}$ is about 90 min. All $S_4O_6^{2-}$ is transferred to SO_4^{2-} with a low concentration of $S_2O_3^{2-}$ (about 2×10^{-5} M) remaining.

When $S_4O_6^{2-}$ is illuminated in the absence of Co(2-TMPyP) (⊙) or if $S_4O_6^{2-}$ is placed in the dark but in the presence of Co(2-TMPyP) with saturated oxygen for 10 h, decomposition of $S_4O_6^{2-}$ is slow. If the catalyst Co(2-TMPyP) (10^{-5} M) is present, the initial rate of $S_4O_6^{2-}$ decomposition is 2×10^{-6} M/min and the production rate of SO_4^{2-} is 8×10^{-6} M/min.

The photocatalytic oxidation of $S_4O_6^{2-}$ by Co(2-TMPyP) can be formulated as follows:

$$2S_4O_6^{2-} + 7O_2 + 6H_2O \rightarrow 8SO_4^{2-} + 12H^+ \quad (1)$$

3.2. The photocatalytic autoxidation of $S_4O_6^{2-}$ by Mn(4-TMPyP) and Fe(2-TMPyP)

Fig. 3 shows the decomposition of tetrathionate at pH 9.0 in the presence of oxygen using

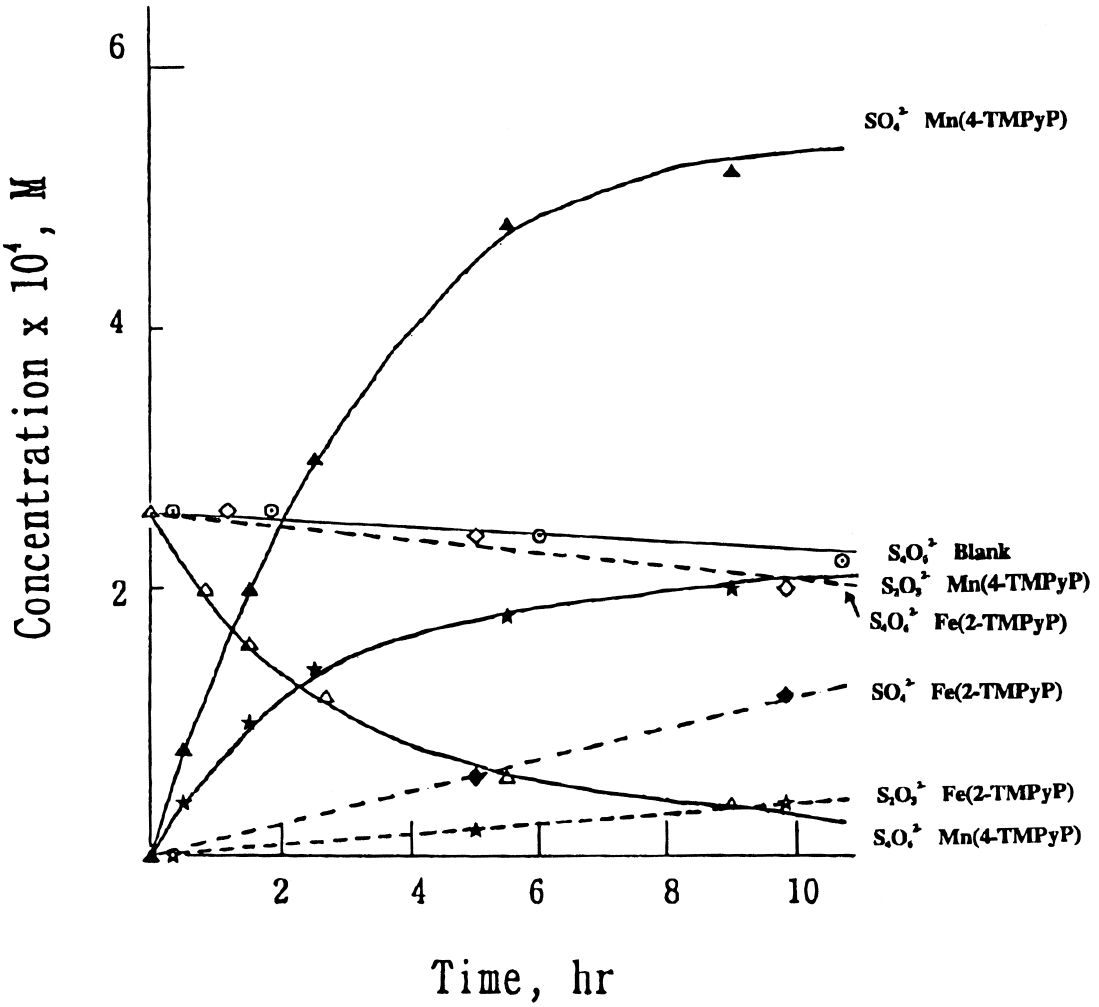

Fig. 3. Concentration of sulfur oxoanions vs. time of oxygen present at pH 9.0 borate buffer solution using 10^{-5} M of Fe(2-TMPyP) and Mn(4-TMPyP), with initial $[S_4O_6^{2-}] = 2.5 \times 10^{-4}$ M under illumination with 419 nm light. (A) (⊙) $[S_4O_6^{2-}]$ without catalyst. (B) Fe(2-TMPyP) present, (◇) $[S_4O_6^{2-}]$, (☆) $[S_2O_3^{2-}]$, (◆) $[SO_4^{2-}]$. (C) Mn(4-TMPyP) present, (△) $[S_4O_6^{2-}]$, (★) $[S_2O_3^{2-}]$, (▲) $[SO_4^{2-}]$.

Table 1
The initial rate of substrate decomposition and product formation for photocatalytic oxidation of $S_4O_6^{2-}$ (2.5×10^{-4} M) and $S_2O_3^{2-}$ (5×10^{-4} M) by various catalysts of porphyrin complexes (10^{-5} M)

Catalyst	Substrate (initial rate, M/min)	Products (initial rate, M/min)
Co(2-TMPyP)	$S_4O_6^{2-}$ (2×10^{-6})	SO_4^{2-} (8×10^{-6})
Mn(4-TMPyP)	$S_4O_6^{2-}$ (1.3×10^{-6})	SO_4^{2-} (2.6×10^{-6})
Fe(2-TMPyP)	$S_4O_6^{2-}$ (8×10^{-8})	SO_4^{2-} (2×10^{-7})
Co(2-TMPyP)	$S_2O_3^{2-}$ (3.3×10^{-6})	SO_4^{2-} (6.0×10^{-6})
Mn(4-TMPyP)	$S_2O_3^{2-}$ (5.0×10^{-8})	SO_4^{2-} (8.5×10^{-8})
Fe(2-TMPyP)	$S_2O_3^{2-}$ (1.3×10^{-6})	SO_4^{2-} (6.3×10^{-7})

Mn(4-TMPyP) and Fe(2-TMPyP) as catalysts. The $S_4O_6^{2-}$ decomposition initial rates are 1.3×10^{-6} M/min, and 8×10^{-8} M/min, respectively (Table 1). $S_2O_3^{2-}$ is an intermediate in the photocatalytic reaction. The final concentrations of SO_4^{2-}, $S_2O_3^{2-}$, and $S_4O_6^{2-}$ after 12 h of illumination are shown in Table 2.

The data indicate that the phenomena of photocatalytic oxidation of $S_4O_6^{2-}$ to SO_4^{2-} by Co(2-TMPyP) under illumination with 419 nm light in a solution of pH 9.0 could be performed efficiently (the $S_4O_6^{2-}$ decomposition initial rates are 2.0×10^{-6} M/min). Mn(4-TMPyP) and Fe(2-TMPyP) also have photocatalytic activity for $S_4O_6^{2-}$ oxidation in pH 9.0 borate aqueous solution, and SO_4^{2-} is the final oxidation product. The photocatalytic oxidation activity of porphyrin complexes follows the trend Co(2-TMPyP) > Mn(4-TMPyP) > Fe(2-TMPyP).

After 12 h of illumination, the percentage of $S_4O_6^{2-}$ transferred to $S_2O_3^{2-}$ by Co(2-TMPyP), Mn(4-TMPyP), Fe(2-TMPyP) are 0%, 44%, and 7%, respectively.

The photocatalytic oxidation can be formulated as follows:

$$S_4O_6^{2-} \xrightarrow[\text{or Fe(2-TMPyP)}]{\text{Mn(4-TMPyP)}} SO_4^{2-} + S_2O_3^{2-} \qquad (2)$$

3.3. The photocatalytic autoxidation of $S_2O_3^{2-}$

Fig. 4 shows the decomposition of thiosulfate at pH 9.0 using Co(2-TMPyP), Fe(2-TMPyP), and Mn(4-TMPyP) as catalysts under illumination with a 419 nm light. The graph shows the decrease of $S_2O_3^{2-}$ and the rise of SO_4^{2-}. Some intermediates are possibly present in the reaction process.

When $S_2O_3^{2-}$ is placed in the dark in the presence of Co(2-TMPyP) or when $S_2O_3^{2-}$ is illuminated in the absence of catalyst (⊙) in saturated oxygen for 10 h, only a small amount of $S_2O_3^{2-}$ is decomposed (Fig. 4). If the catalyst Co(2-TMPyP)(10^{-5} M) is present, the $S_2O_3^{2-}$ tranferred to SO_4^{2-} (○) is fast with an initial rate of $S_2O_3^{2-}$ decomposition (●) of 3.3×10^{-6} M/min, and SO_4^{2-} production rate of 6.0×10^{-6} M/min.

Fig. 4 also shows the decomposition of thiosulfate at pH 9.0 in the presence of oxygen with Fe(2-TMPyP) (▲) and Mn(4-TMPyP) (■) as

Table 2
The photocatalytic oxidation products of $S_4O_6^{2-}$ (2.5×10^{-4} M) and $S_2O_3^{2-}$ (5×10^{-4} M) by various catalysts of porphyrin complexes after 12 h of illumination under 419 nm light

Catalyst (survived)[a]	Substrate	Products, intermediate, and substrate (final concentration)
Co(2-TMPyP) 60%	$S_4O_6^{2-}$	SO_4^{2-} (1×10^{-3} M), $S_2O_3^{2-}$ (0.0 M), $S_4O_6^{2-}$ (0.0 M)
Mn(4-TMPyP) 100%	$S_4O_6^{2-}$	SO_4^{2-} (5.6×10^{-4} M), $S_2O_3^{2-}$ (2.2×10^{-4} M), $S_4O_6^{2-}$ (0.0 M)
Fe(2-TMPyP) 100%	$S_4O_6^{2-}$	SO_4^{2-} (1.3×10^{-4} M), $S_2O_3^{2-}$ (3.5×10^{-5} M), $S_4O_6^{2-}$ (2.0×10^{-4} M)
Co(2-TMPyP) 65%	$S_2O_3^{2-}$	SO_4^{2-} (1×10^{-3} M), $S_2O_3^{2-}$ (0.0 M)
Fe(2-TMPyP) 100%	$S_2O_3^{2-}$	SO_4^{2-} (3.5×10^{-4} M), $S_2O_3^{2-}$ (2.5×10^{-4} M)
Mn(4-TMPyP) 100%	$S_2O_3^{2-}$	SO_4^{2-} (1.4×10^{-4} M), $S_2O_3^{2-}$ (4.0×10^{-4} M)

[a] Percentage of catalyst survived after 12 h illumination in the presence of substrate.

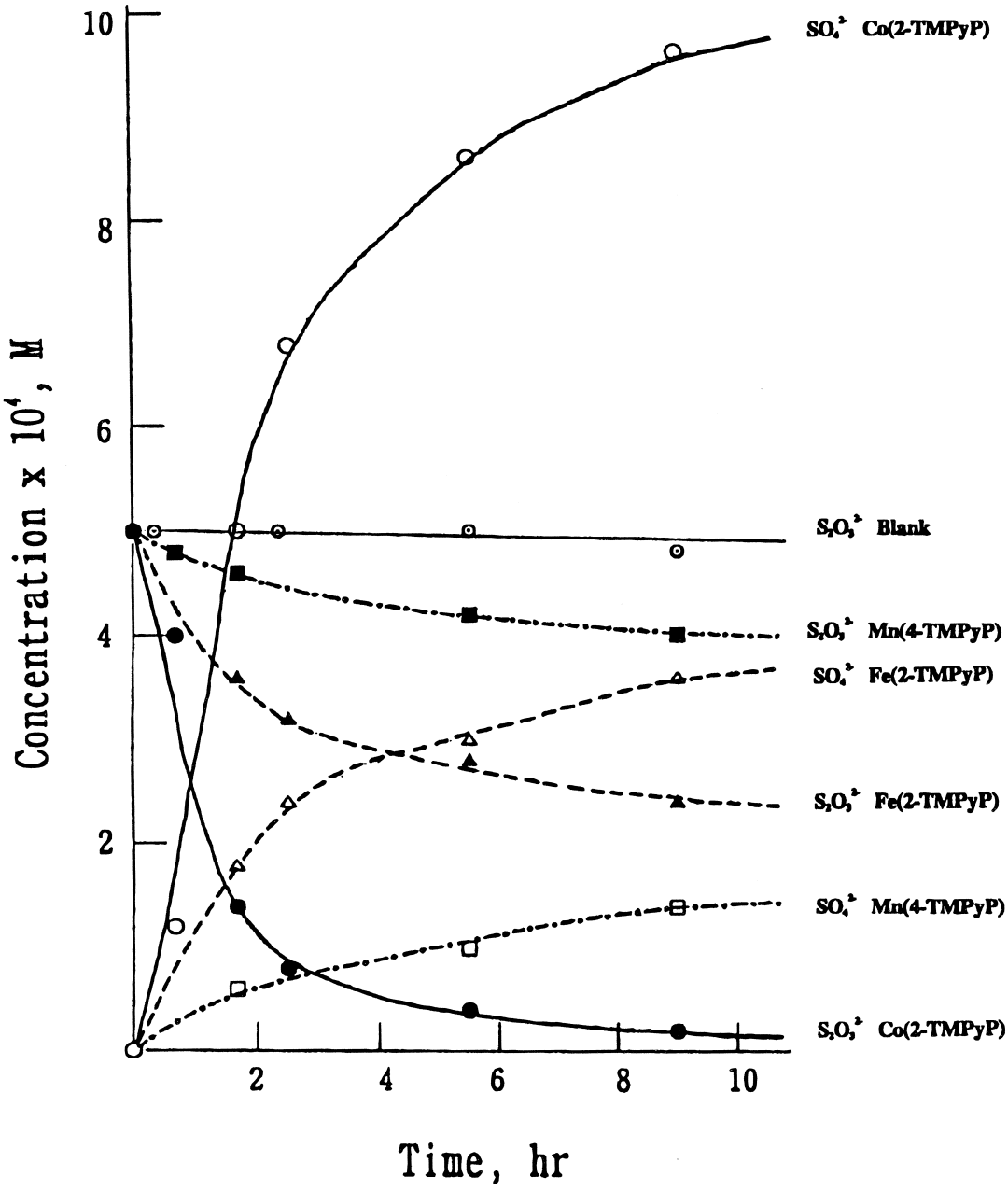

Fig. 4. Concentration of sulfur oxoanions vs. time of oxygen present at pH 9.0 borate buffer solution using 10^{-5} M of Fe(2-TMPyP), Co(2-TMPyP), and Mn(4-TMPyP), $[S_2O_3^{2-}] = 5.0 \times 10^{-4}$ M under illumination with 419 nm. (A) (⊙) $[S_2O_3^{2-}]$ without catalyst. (B) Fe(2-TMPyP) present, (▲) $[S_2O_3^{2-}]$, (△) $[SO_4^{2-}]$. (C) Mn(4-TMPyP) present, (■) $[S_2O_3^{2-}]$, (□) $[SO_4^{2-}]$. (D) Co(2-TMPyP) present, (●) $[S_2O_3^{2-}]$, (○) $[SO_4^{2-}]$.

catalysts. $S_2O_3^{2-}$ decomposition initial rates are 1.3×10^{-6} M/min and 5.0×10^{-8} M/min, respectively. Some intermediates may exist in the reaction process from the species concentration calculation, but are completely transferred to SO_4^{2-} after a long time of illumination.

The data indicate that the phenomena of photocatalytic oxidation of $S_2O_3^{2-}$ to SO_4^{2-} by

Co(2-TMPyP) under illumination with 419 nm in a solution at pH 9.0 could be performed effect. Fe(2-TMPyP) and Mn(4-TMPyP) also have photocatalytic activity for $S_2O_3^{2-}$ oxidation in pH 9.0 borate aqueous solution. SO_4^{2-} is the final product. The trend in photocatalytic oxidation activity of the porphyrin complexes is Co(2-TMPyP) > Fe(2-TMPyP) > Mn(4-TMPyP). After 12 h illumination, the undecomposed percentage of $S_2O_3^{2-}$ by Co(2-TMPyP), Fe(2-TMPyP), Mn(4-TMPyP) are 0%, 50%, and 80%, respectively.

3.4. The properties of catalysts

The absorption spectrum of Fe(2-TMPyP) (————), Mn(4-TMPyP)(- - -), and Co(2-TMPyP) (. . .) at pH 9.0 buffer aqueous solution are shown in Fig. 5. The spectra show that the three porphyrin complexes have high absorption coefficients at 419 nm. The Soret band of Co(2-TMPyP), Fe(2-TMPyP), Mn(4-TMPyP) are at 423 nm, 409 nm, and 463 nm respectively. The molar absorptivity of Co(2-TMPyP), Fe(2-TMPyP), Mn(4-TMPyP) in pH 9.0 buffer solution at 419 nm are 2.2×10^5, 9.1×10^4, 2.8×10^4, respectively.

Fig. 6 shows the cyclic voltammograms of Fe(2-TMPyP), Mn(4-TMPyP), Co(2-TMPyP) at pH 9.0 buffer solution. The redox couples of Fe(III/II) (2-TMPyP) [23,24] and Mn(III/II)(4-TMPyP) [25,26] have close values of formal potential, and the redox couple of Mn(III/IV)(4-TMPyP) and Co(II/III)(2-TMPyP) [27,28] have similar values of formal potential. The redox couple of Co(II/I)(2-TMPyP) is more positive than Fe(II/I)(2-TMPyP), and Fe(III/IV)(2-TMPyP) is more

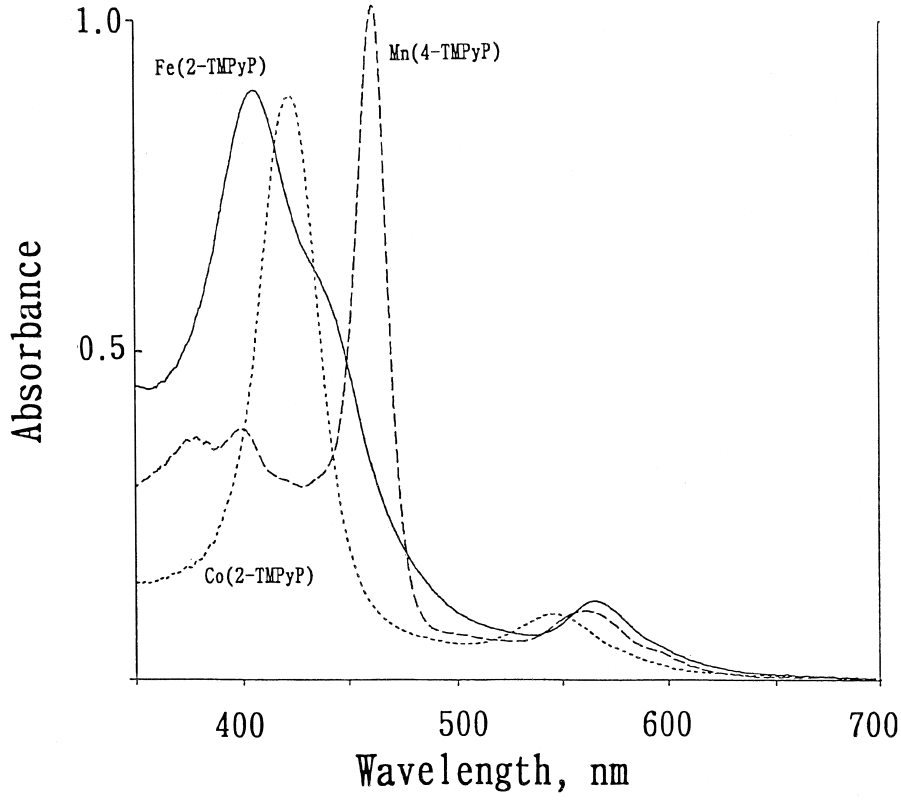

Fig. 5. Absorption spectrum of (a) 9.0×10^{-6} M Fe^{III}(2-TMPyP) (————), (b) 3.5×10^{-6} M Co^{II}(2-TMPyP) (. . .), (c) 1.1×10^{-5} M Mn^{III}(4-TMPyP) (- - -), at pH 9.0 buffer solution.

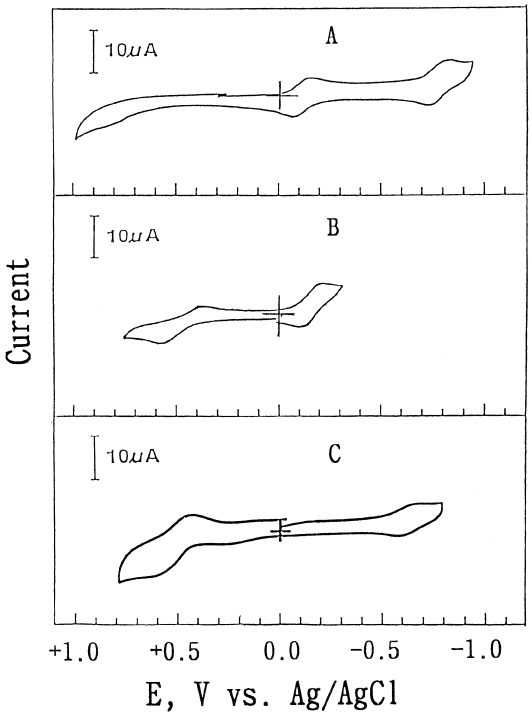

Fig. 6. Cyclic voltammograms of (A) 2.5×10^{-4} M Fe(2-TMPyP), (B) 5.0×10^{-4} M Mn(4-TMPyP), (C) $2.0\times10-4$ M Co(2-TMPyP), in pH 9.0 buffer solution. Scan rate 0.1 V/s.

positive than Mn(III/IV)(4-TMPyP) and Co(II/III)(2-TMPyP). The formal potentials of the different redox couples of porphyrin complexes are summarized in Table 3.

Fig. 7 shows the absorption spectra of Co(2-TMPyP) at pH 9.0 buffer solution with different concentrations of $S_4O_6^{2-}$. As the concentration

Table 3
The formal potentials of various porphyrin complexes at pH 9.0 borate buffer solution

	[M(IV/III)P]	[M(III/II)P]	[M(II/I)P]
Fe(2-TMPyP)	+0.57[a]	−0.14	−0.76[b]
Mn(4-TMPyP)	+0.47	−0.17	No[c]
Co(2-TMPyP)	No	+0.48	−0.61[d]

[a] Refs. [23,29], data taken from spectroelectrochemical method.
[b] Ep_{cat} for the electrocatalytic reduction of $S_4O_6^{2-}$ is −0.80 V (vs. Ag/AgCl).
[c] Ep_{cat} for the electrocatalytic reduction of $S_4O_6^{2-}$ is −0.72 V (vs. Ag/AgCl).
[d] Ep_{cat} for the electrocatalytic reduction of $S_4O_6^{2-}$ is −0.60 V (vs. Ag/AgCl).

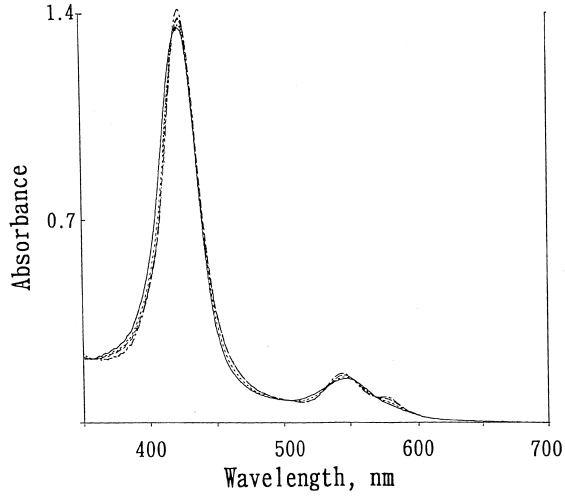

Fig. 7. Absorption spectra change of 3.8×10^{-6} M Co^{II}(2-TMPyP) at pH 9.0 borate buffer in the presence of different $S_4O_6^{2-}$ concentration. (a) 0.0 M; (b) 4.0×10^{-4} M; (c) 1.6×10^{-3} M; (d) 3.3×10^{-3} M.

of $S_4O_6^{2-}$ increases gradually from 0 M to 3.3×10^{-3} M, the new spectrum appear with isosbestic points at 356, 418, 503, 532, 553, 570 nm. There is coordination or interaction between Co(2-TMPyP) and $S_4O_6^{2-}$, but no obvious interaction between Co(2-TMPyP) and $S_2O_3^{2-}$ under the same conditions.

The result can be expressed as follows:

$$Co^{II}(2-TMPyP) + S_4O_6^{2-} \rightarrow Co^{II}(2-TMPyP)\left(S_4O_6^{2-}\right) \quad (3)$$

3.5. Catalysts concentration and the photocatalytic autoxidation

The absorption spectra show that Co(2-TMPyP) has higher molar absorption at 419 nm. When the photocatalytic autoxidation of $S_4O_6^{2-}$ was performed with the catalysts at the same absorbance at 419 nm ($A = 1.0$), the trend in photocatalytic oxidation is Mn(4-TMPyP) > Co(2-TMPyP) > Fe (2-TMPyP), because the concentration of Mn(4-TMPyP) is 3.3 times that of Fig. 3 and the concentration Co(2-TMPyP) is 0.4 times that of Fig. 2. The initial rates of

SO_4^{2-} production are 9.4×10^{-6} M/min, 3.2×10^{-6} M/min and 2.6×10^{-7} M/min for the catalysts Mn(4-TMPyP), Co(2-TMPyP), and Fe(2-TMPyP) ($A_{419} = 1.0$), respectively.

In the case of the photocatalytic autoxidation of $S_2O_3^{2-}$ with the catalysts at the same absorbance at 419 nm ($A = 1.0$), the results show that the trend in photocatalytic oxidation is Co(2-TMPyP) > Fe(2-TMPyP) > Mn(4-TMPyP) (Fig. 8).

For the photocatalytic reaction:

$$S_4O_6^{2-} \rightarrow SO_4^{2-} \quad (4)$$

the catalytic activity of Co(2-TMPyP) and Mn(4-TMPyP) ≫ Fe(2-TMPyP).

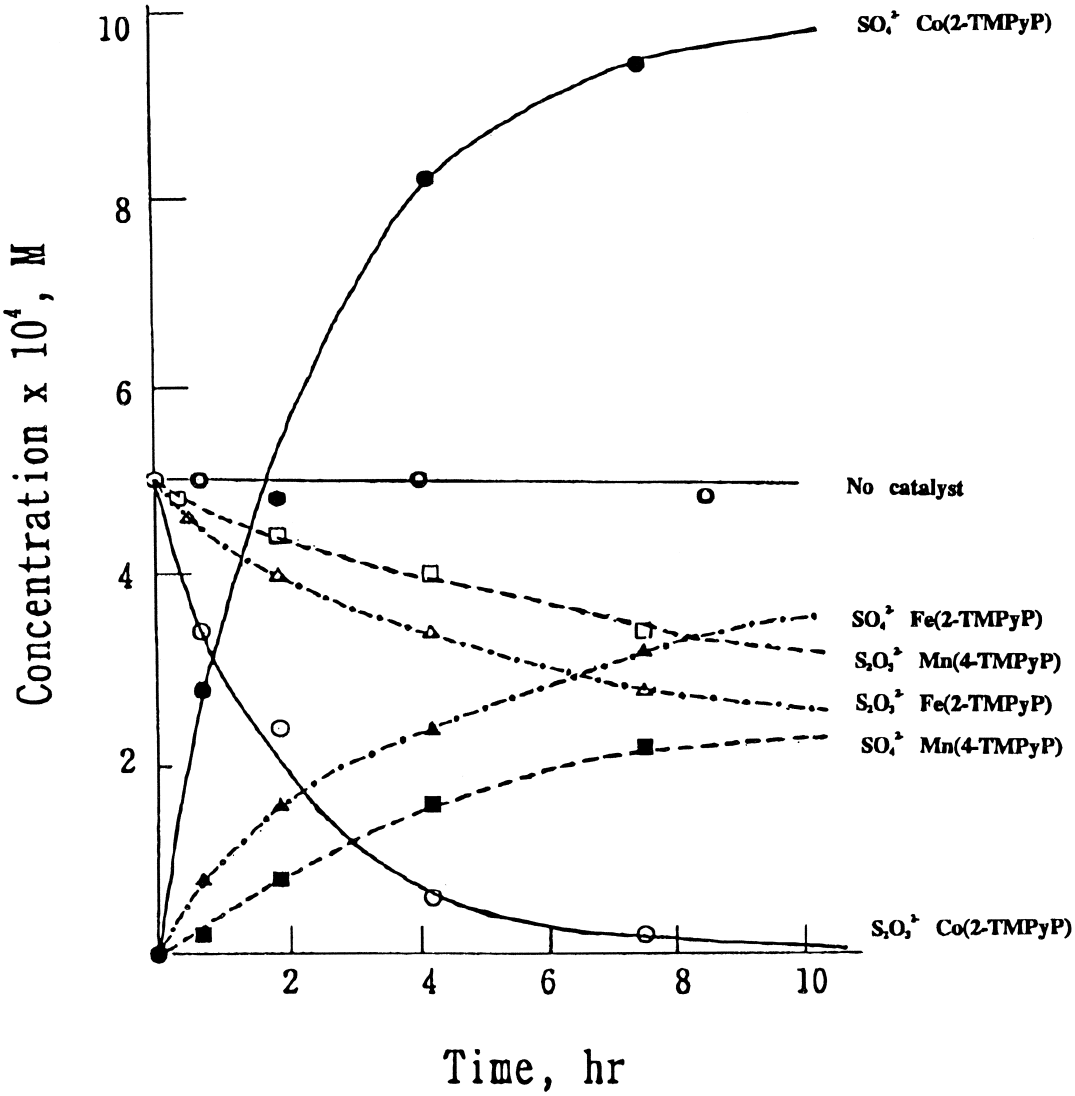

Fig. 8. Concentration of sulfur oxoanions vs. time of oxygen present at pH 9.0 borate buffer solution with $A_{419} = 1.0$ of Fe(2-TMPyP), Co(2-TMPyP), and Mn(4-TMPyP), with initial $[S_2O_3^{2-}] = 5.0 \times 10^{-4}$ M under illumination with 419 nm light. (A) (⊙) $[S_2O_3^{2-}]$ without catalyst. (B) Fe(2-TMPyP) present, (▲) $[S_2O_3^{2-}]$, (△) $[SO_4^{2-}]$. (C) Mn(4-TMPyP) present, (■) $[S_2O_3^{2-}]$, (□) $[SO_4^{2-}]$. (D) Co(2-TMPyP) present, (●) $[S_2O_3^{2-}]$, (○) $[SO_4^{2-}]$.

For the photocatalytic reaction:

$$S_2O_3^{2-} \rightarrow SO_4^{2-} \quad (5)$$

the trend in catalytic activity is Co(2-TMPyP) > Fe(2-TMPyP) > Mn(4-TMPyP).

3.6. Effect of substrate concentration on the photocatalytic reaction

Figs. 9 and 10 show the photocatalytic autoxidation of $S_4O_6^{2-}$ and $S_2O_3^{2-}$ with constant amount of Co(2-TMPyP) and varying the initial concentration of substrates.

The production rate of SO_4^{2-} is directly proportional to the initial concentration of substrate.

Fig. 11 shows the photocatalytic autoxidation of $S_4O_6^{2-}$ by varying the concentration of Mn(4-TMPyP). In all the different concentrations of Mn(4-TMPyP) performed, SO_4^{2-} production rate is directly proportional to the concentration of Mn(4-TMPyP).

Fig. 12 shows the photocatalytic autoxidation of 5.0×10^{-4} M, 2.5×10^{-4} M, 1.2×10^{-4} M, and 0.6×10^{-4} M $S_4O_6^{2-}$ by constant amount of Mn(4-TMPyP). For initial concentra-

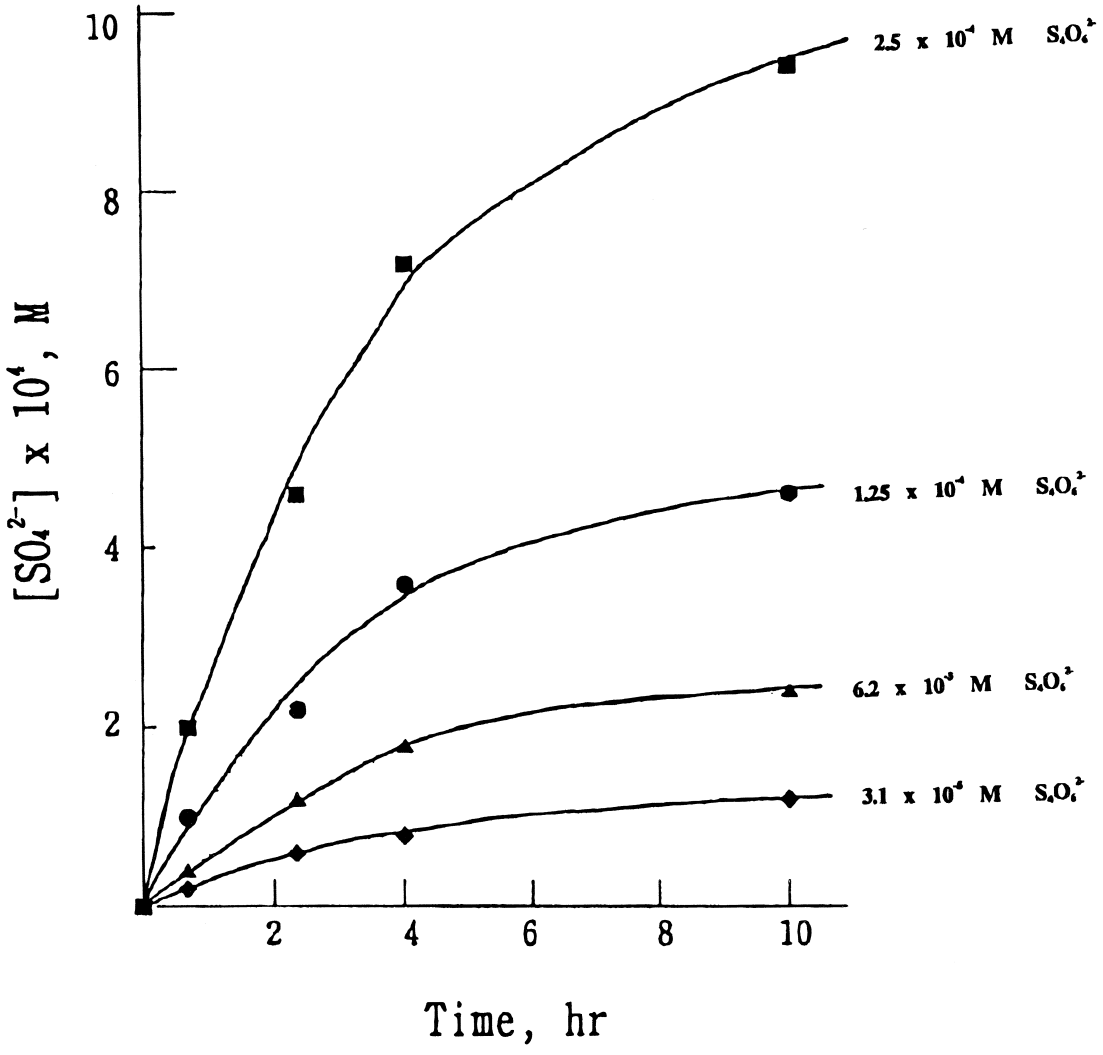

Fig. 9. Concentration of $[SO_4^{2-}]$ vs. time of oxygen present at pH 9.0 borate buffer solution using 8×10^{-6} M of Co(2-TMPyP) and illumination with 419 nm light. $[S_4O_6^{2-}] = (\blacksquare)\ 2.5 \times 10^{-4}$ M; $(\bullet)\ 1.2 \times 10^{-4}$ M; $(\blacktriangle)\ 0.6 \times 10^{-4}$ M; $(\blacklozenge)\ 0.3 \times 10^{-4}$ M.

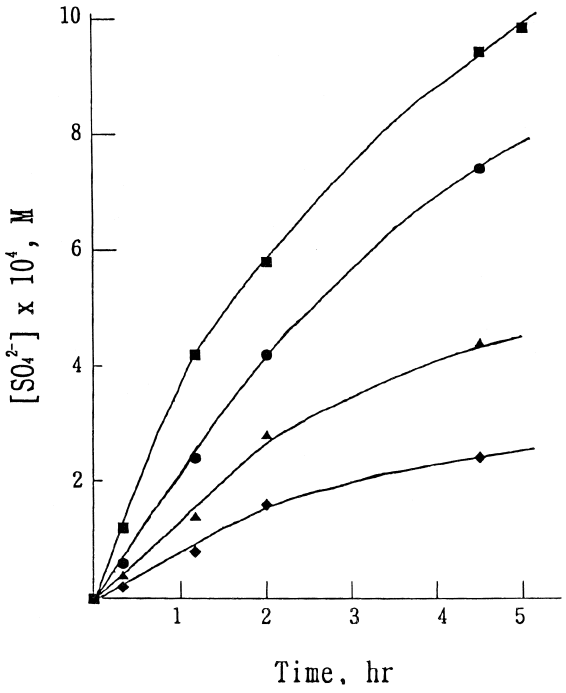

Fig. 10. Concentration of $[SO_4^{2-}]$ vs. time of oxygen present at pH 9.0 borate buffer solution using 8×10^{-6} M of Co(2-TMPyP) under illumination with 419 nm light. $[S_2O_3^{2-}]=$ (■) 5.0×10^{-4} M; (●) 2.5×10^{-4} M; (▲) 1.2×10^{-4} M; (◆) 0.6×10^{-4} M.

tions of 1.2×10^{-4} M, 0.6×10^{-4} M, SO_4^{2-} and $S_2O_3^{2-}$ production concentration is increasingly dependent to the concentration of substrate. For initial concentrations of 5.0×10^{-4} M, 2.5×10^{-4} M, SO_4^{2-}, production concentration is increasingly independent to the concentration of substrate.

3.7. The photocatalytic autoxidation mechanisms

Products analysis by ion chromatography identified $S_2O_3^{2-}$ as the intermediate of photocatalytic reaction of $S_4O_6^{2-}$ by Co(2-TMPyP), Mn(4-TMPyP) and Fe(2-TMPyP). Photodecomposition of $S_4O_6^{2-}$ follows a stepwise decomposition and oxidation to SO_4^{2-} by oxygen as shown in Eq. (6).

$$S_4O_6^{2-} \rightarrow S_2O_3^{2-} \rightarrow SO_3^{2-} \rightarrow SO_4^{2-} \qquad (6)$$

I have reported in previous papers that the electrocatalytic reduction of $S_4O_6^{2-}$ to $S_2O_3^{2-}$ by porphyrin complexes [24,25,27] is through the Fe(I)(2-TMPyP) and Co(I)(2-TMPyP) species. For Mn(4-TMPyP), catalytic wave potential is after the Mn(III/II)(4-TMPyP) redox couple with a $Ep_{cat} = -0.72$ V(vs. Ag/AgCl). Electrocatalytic peak potential for transferring $S_4O_6^{2-}$ to $S_2O_3^{2-}$ at pH 9.0 is -0.60 V, -0.72 V, and -0.80 V by Co(2-TMPyP), Mn(4-TMPyP), Fe(2-TMPyP) as catalyst, respectively (Table 3). The electrocatalytic reaction peak potentials are consistent with the photocatalytic decomposition rate of $S_4O_6^{2-}$. The coordination or interaction between Co^{II}(2-TMPyP) and $S_4O_6^{2-}$ may enhance the photocatalytic autoxidation of $S_4O_6^{2-}$.

I have recently shown that the electrocatalytic oxidation of $S_2O_3^{2-}$ and $S_4O_6^{2-}$ by Co(2-

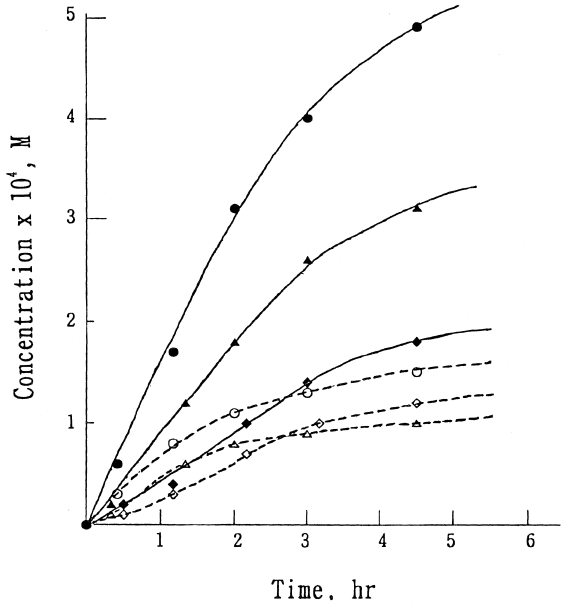

Fig. 11. Concentration of sulfur oxoanions vs. time of oxygen present at pH 9.0 borate buffer solution with 2.5×10^{-4} M $S_4O_6^{2-}$ under illumination with 419 nm light. [Mn(4-TMPyP)]= (A) 2.5×10^{-5} M, (○) $[S_2O_3^{2-}]$, (●) $[SO_4^{2-}]$, (B) 1.2×10^{-5} M, (△) $[S_2O_3^{2-}]$, (▲) $[SO_4^{2-}]$, (C) 0.6×10^{-5} M, (◇) $[S_2O_3^{2-}]$, (◆) $[SO_4^{2-}]$.

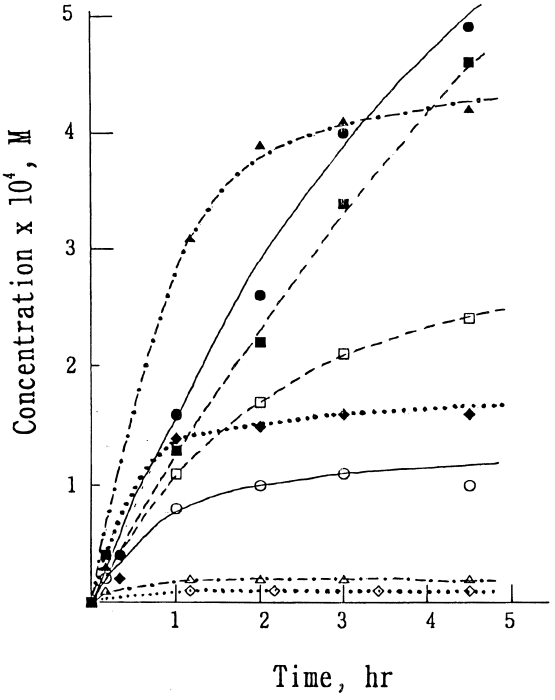

Fig. 12. Concentration of sulfur oxoanions vs. time of oxygen present at pH 9.0 borate buffer solution using 2.5×10^{-5} M Mn(4-TMPyP) under illumination with 419 nm light. $[S_4O_6^{2-}]=$ (A) 5.0×10^{-4} M, (□) $[S_2O_3^{2-}]$, (■) $[SO_4^{2-}]$, (B) 2.5×10^{-4} M, (○) $[S_2O_3^{2-}]$, (●) $[SO_4^{2-}]$. (C) 1.2×10^{-4} M, (△) $[S_2O_3^{2-}]$, (▲) $[SO_4^{2-}]$, (D) 0.6×10^{-4} M, (◇) $[S_2O_3^{2-}]$, (◆) $[SO_4^{2-}]$.

TMPyP) [27] is through the Co(III)(2-TMPyP) species with obvious activity. The electrocatalytic oxidation of $S_2O_3^{2-}$ is not very active by Fe(2-TMPyP) and Mn(4-TMPyP) in the cyclic voltammetry time scale. The electrocatalytic reaction results are consistent with the photocatalytic decomposition rate of $S_2O_3^{2-}$.

When $S_2O_3^{2-}$ transfered to SO_3^{2-}, then catalytic autoxidation of SO_3^{2-} by porphyrin complexes is easy in the presence of oxygen [25,30].

4. Conclusion

The water-soluble porphyrin complexes Fe(2-TMPyP), Mn(4-TMPyP), and Co(2-TMPyP) exhibit catalytic activity under irradiation with a 419 nm visible light. Under conditions of photocatalysis and autoxidation, $S_4O_6^{2-}$ decomposes to thiosulfate and sulfate. Co(2-TMPyP) completely converts $S_4O_6^{2-}$ to SO_4^{2-}, while Fe(2-TMPyP) and Mn(4-TMPyP) are only partially effective, thus producing $S_2O_3^{2-}$.

Acknowledgements

This work was supported by the National Science Council of the Republic of China.

References

[1] A. Kotronarou, M.R. Hoffmann, Environ. Sci. Technol. 25 (1991) 1153.
[2] W. Spiller, D. Wohrle, G. Schulz-Ekloff, W.T. Ford, G. Schneider, J. Stark, J. Photochem. Photobiol. A Chem. 95 (1996) 161.
[3] B.W. Henderson, T.J. Dougherty, Photochem. Photobiol. 55 (1992) 145.
[4] G. Jori, J. Photochem. Photobiol. A Chem. 62 (1992) 371.
[5] C.E. Hoyle, D.E. Hutchens, S.F. Thames, Macromol. Chem. 22 (1989) 3913.
[6] H. Deng, H. Mao, B. Liang, Y. Shen, Z. Lu, H. Xu, J. Photochem. Photobiol. A Chem. 99 (1996) 71.
[7] Y. Kaneko, Y. Nishimura, T. Arai, H. Sakuragi, K. Tokumaru, D. Matsunaga, J. Photochem. Photobiol. A Chem. 89 (1995) 37.
[8] J.D. Spikes, J.E. van Lier, J.C. Bommer, J. Photochem. Photobiol. A Chem. 91 (1995) 193.
[9] G. Schneider, D. Wohrle, W. Spiller, J. Stark, G. Schulz-Ekloff, Photochem. Photobiol. 60 (1994) 333.
[10] X.-F. Zhang, H.-J. Xu, J. Photochem. Photobiol. A Chem. 91 (1995) 193.
[11] D. Schlettwein, M. Kaneko, A. Yamada, D. Wohrle, N.I. Jaeger, J. Phys. Chem. 95 (1991) 1748.
[12] J.R. Darwent, P. Douglas, A. Harriman, G. Porter, M.-C. Richoux, Coord. Chem. Rev. 44 (1982) 83.
[13] M. Fischer, P. Warneck, J. Phys. Chem. 100 (1996) 15111.
[14] U. Deister, P. Warneck, J. Phys. Chem. 94 (1990) 2191.
[15] A. Ansari, J. Peral, X. Domenech, R. Rodriguez-Clemente, A. Roig, E. Molins, J. Photochem. Photobiol. A Chem. 87 (1995) 121.
[16] B.C. Faust, M.R. Hoffmann, D.W. Bahnemann, J. Phys. Chem. 93 (1989) 6371.
[17] A.P. Hong, D.W. Bahnemann, M.R. Hoffmann, J. Phys. Chem. 91 (1987) 6245.
[18] I.B. Rufus, B. Viswanathan, V. Ramakrishnan, J.C. Kuriacose, J. Photochem. Photobiol. A Chem. 91 (1995) 63.
[19] C. Brandt, R. van Eldik, Chem. Rev. 95 (1995) 119.
[20] P. Hambright, T. Gore, M. Burton, Inorg. Chem. 15 (1976) 2314.

[21] J. Davila, A. Harriman, M.-C. Richoux, L.R. Milgrom, J. Chem. Soc., Chem. Commun., 1987, p. 525.
[22] A.D. Adler, F.R. Longo, F. Kampas, J. Kim, J. Inorg. Nucl. Chem. 32 (1970) 2443.
[23] S.-M. Chen, P.-J. Sun, Y. Oliver Su, J. Electroanal. Chem. 294 (1990) 151.
[24] S.-M. Chen, Inorg. Chim. Acta 244 (1996) 155.
[25] S.-M. Chen, J. Electroanal. Chem. 407 (1996) 123.
[26] C.-Y. Lin, Z.-F. Lin, T.-M. Hseu, Y. Oliver Su, J. Chin. Chem. Soc. 37 (1990) 335.
[27] S.-M. Chen, J. Electroanal. Chem. 432 (1997) 101.
[28] S.H. Cheng, Y. Oliver Su, Inorg. Chem. 33 (1994) 5847.
[29] S.-M. Chen, Y. Oliver Su, J. Chem. Soc., Chem. Commun., 1990, p. 491.
[30] S.-M. Chen, J. Mol. Catal. A Chem. 112 (1996) 277.